A snapshot of the Northern Apennines (Italy) seismicity, merging catalogue and new seismic data

D. Piccinini[1)], N. Piana Agostinetti[1)], P. Roselli[1)], M. Ibs-von Seht[2)] & T. Braun[1)]

[1)] Istituto Nazionale di Geofisica e Vulcanologia, Roma, Italy

[2)] Federal Institute for Geosciences and Natural Resources, Hannover, Germany

Keywords: Northern Apennines, seismicity, focal mechanisms, stress field

Abstract

In this paper we present the seismicity analysis of a small sector of the Northern Apennines in terms of spatio-temporal distribution, merging data from the Italian seismic bulletin with new data collected by temporal seismic networks. Our attention is focused on the region enclosed between Toscana, Umbria, Marche and Emilia-Romagna. This area is mainly characterized by a diffuse seismicity, partly clustered in small sequences ($M_w < 4.7$). Improved seismicity locations, together with stress field analysis allows to characterize the manner of seismogenic stress release in the area. Two regions of significantly different seismic release behavior could be distinguished: (i) the inner/western part (Tuscan side) of the study area, where seismicity is clustered at shallow depths (<18 km) and where strong earthquakes occurred in the past, (ii) the outer(eastern) part (Marche side), where the seismicity is diffuse across all of the crustal volume, reaching depths of down to 30 km.

Along the Apenninic chain, seismicity is nearly absent inside well defined zones. In our opinion, these peculiarities of seismicity release could be related to the heterogeneity of crustal volume and to the transition between Tyrrhenian and Adriatic domains.

1. Introduction

In the last decades, Central Italy was the setting for a considerable number of moderate earthquakes with magnitudes up to M=6 (Gubbio, 1984; Colfiorito, 1997/1998; Gualdo Tadino, 1998, Ciaccio et al., 2005). Nearly all major events occurred on SW dipping (40°-50°) normal faults, an observation that gives one of the main evidences for the predominant extensional stress regime of the Northern Apennines. Analysis of seismic reflection profiles revealed that the crustal structure of the Northern Apennines is characterized by a set of NE-dipping, low angle normal faults (LANF). As recently demonstrated, the easternmost of these LANFs, the Alto Tiberina Fault (hereinafter ATF), shows a strong microseismic activity (Boncio et al., 2000, Collettini and Barchi et al., 2002, Piccinini et al. 2003, Chiaraluce et al. 2007).

The topography of the ATF is well imaged by passive seismic observations up to *Città di Castello*, the north-western limit of the microseismic activity. On the adjacent northern part, towards the *Casentino* area, microseismicity is virtually absent, but evaluation of reflection

seismic profiles near *Sansepolcro* (Barchi et al., 1998) and *Pieve Santo Stefano* (Ciaccio et al., 2007) give evidence for a continuation of the ATF towards north for at least 15 km. The continuation of the ATF towards NW has been proposed by Boncio et al. (2000) who postulated the aggregation of the ATF with faults of the Northern Apennines along the so called Etrurian Fault System (EFS) passing along the *Casentino* area (dashed red line in figure 1).

In the present study we review and analyze the seismicity distribution occurring in a sector of the Northern Apennines including new data recorded by temporary local seismic networks. We correlate different phenomena of seismic stress release such as background microseismicity (M<3.5), moderate seismic sequences (3.5<M<5.5), and strong historical earthquakes (M>5.5).

2. Tectonic setting of the study area

The Northern Apennines are composed of a NE-verging thrust-fold belt, formed as the result of the collision between the European continental margin (Sardinia-Corsica block) and the Adriatic lithosphere (e.g. Alvarez, 1972; Reutter et al., 1980). At the present day, this portion of the belt is subject to active crustal extension, accompanied by moderate to large normal faulting earthquakes that occur on NW-trending SW-dipping normal faults with lengths of usually less than 10 km (Deschamps et al., 1984; Westaway et al., 1989; Haessler et al., 1988, Boncio and Lavecchia, 2000). Focal mechanisms of seismic events and borehole break-outs (Montone et al., 2004) reveal a regional stress field with a nearly vertical σ1 axis and a NE-trending sub-horizontal σ3 axis, and an extensional strain rate in the order of 2.5 mm/yr (Hunstad et al., 2003). Recently, the interpretation of seismic reflection profiles provided by the CROP03-NVR seismic active experiment (CROsta Profonda Project Near Vertical Reflection; Pialli et al., 1998) showed that a significant amount of extension within the brittle upper crust is accommodated by a set of east-dipping low angle normal faults associated with high-angle antithetic structures. Following Boncio et al. (2000), these structures developed during the last ca. 3.5 Ma (Late Pliocene-Quaternary) and formed graben and half-graben systems.

. Its geometry is clearly imaged in seismic reflection profiles (Barchi et al., 1998) and is consistent with movements along an east-dipping extensional fault. This main active fault is known as the Alto Tiberina Fault (ATF) and can be imaged continuously for at least 60 km from

Sansepolcro to Perugia (figure 1). Recent studies of the microseismic activity of the ATF, performed by Piccinini et al. (2003) and Chiaraluce et al. (2007), showed that in the area between Sansepolcro and Città di Castello the seismicity seems to be almost absent.

In the past, the study area was hit by strong earthquakes. Following the CFTI on-line database (Guidoboni et al., 2007) we could cluster the historical events for *the S. Sofia* area as represented by four historical strong earthquakes with 5.8 < Me < 6.1, in 1279, 1584, 1661 and 1768. During the 20th century a Me = 5.9 struck the same area (1918/11/10). The central part of the study area (*Sansepolcro*) was hit by numerous strong and moderate events with maximum equivalent magnitude Me = 6.3 (1781). The last moderate event reported in the catalogue is represented by the 1917 Me = 5.9 event which struck the area close *Città di Castello*. In the south-eastern part the historical seismicity is represented by the two events located in the *Gualdo Tadino* area in 1747 (Me = 5.8) and in 1751 (Me = 6.3) which reaches the maximum value of intensity (X).

3. Dataset and analysis procedures

The study area (figure 1), hereinafter called Upper Tiber Valley (UTV), belongs to the Northern Apennines and is confined in the NE by the Tuscan-Emilian Apennines, in the W by the Arno Valley area and in the SE by the Umbria-Marche Apennines. In order to better understand the location and the time evolution of the local seismicity, two permanent seismic networks and a number of temporary seismic deployments were carried out inside the UTV. In this study, we analyze in detail the local seismicity recorded by six different datasets (Figure 1): (1) the Italian Seismic Network (ISN), (2) the Marche Regional Seismic Network (RSM), (3) the Central Apennines Experimental Seismic Array (CAESAR-1), (4) the Arno Valley Experimental Seismic Array (AVESA), (5) the Linear Array for Site Effect Studies (LASES), and (6) a small network north of Sansepolcro (CAESAR-2). Data from the ISN belong to two different sources: (i) the Catalogue of the Seismicity of Italy (CSI 1.1, Chiarabba et al., 2005), which reports the Italian seismicity between 1981-2002, and (ii) the seismic bulletin of the Istituto Nazionale di Geofisica e Vulcanologia (INGV), which contains phases and localizations of earthquakes that occurred along the Italian peninsula between 2003 and present. The RSM dataset contains phases recorded at 16 seismic stations deployed across the Marche region. Due to the proximity of the study area to the Marche region, seismic phases from the RSM catalogue have been merged to the

temporary deployment dataset. The CAESAR-1 deployment (October 2002-March 2003), included five seismic stations equipped with Mars88 digitizers and short period three-component seismometers (Mark L4-3D) and was aimed to better define the epicenter of the diffuse seismicity located between the Upper Tiber Valley and the Casentino area. AVESA (September – October 2005) used an array of 12 stations equipped with MarsLite digitizers and Lennartz Le3d-5s (Braun et al., 2006). LASES (May 2005-November 2005) aimed to perform site effect studies in the Upper Tiber Valley, using eight seismic stations with Le5s-3D and CMG-40T broadband seismic sensors (Azzara et al., 2006). The CAESAR-2 (October 2002 - March 2003) array comprised six seismic stations and was deployed in the same area as the CAESAR-1 network. Stations were equipped with Mark-L4D sensor and MARS-88 digitizers. Datasets from the above mentioned permanent and temporary deployments have been included to obtain a homogeneous dataset of the seismicity in the study area.

We analyzed the complete dataset following classical methods for local earthquakes analysis. To better constrain earthquake locations, we first computed a minimum 1-D velocity model using the VELEST code of Kissling et al. (1994), by simultaneously inverting hypocentral and velocity parameters. Afterwards, Hypoellipse (Lahr, 1989) was used to locate the seismicity in the study area. Finally, we used Hypo-DD (Waldhauser and Ellsworth, 2000) to refine the localization of the individual seismic sequence or cluster. For each sequence, we computed focal mechanisms solutions using FPFIT (Reasenberg and Oppenheimer, 1985). An inversion of the resulting fault plane solutions was performed using Michael's method (Michael, 1984) to compute direction and plunge of the principal stress axes.

In order to calculate a relevant start velocity model for the location procedure, data from the CSI 1.1 catalogue were used. The CSI 1.1 contains arrival times of all available stations of the Italian Seismic Network and of all regional networks operating in Italy (Chiarabba et al., 2005). We extracted 3644 events with epicenter inside the area of interest, associated P- and S-wave arrivals 70 stations, located the events by Hypoellipse and finally retrieved a detailed 1-D velocity model to be used for the subsequent relocation process. A subset of the complete dataset was formed by selecting 543 events with horizontal locations errors (ERH) less than 2 km and vertical location errors (ERZ) less than 3 km. The subset comprised 6440 P- and S-phases and was used to compute the minimum 1-D velocity model of the area. The result of the VELEST inversion (Table 1) produced a final unweighted RMS residual of 0.16 s which corresponds to an RMS

reduction of about 60%. The upper crustal volume is well resolved down to a depth 8 km, with more than 2000 rays passing through. Although the area investigated in the present study is large and geologically heterogeneous, the found P-wave velocities are in accordance with those reported by Piccinini et al. (2003) and they are also consistent with similar values derived from drilling logs and laboratory experiments (Bally et al., 1986). The V_P/V_S ratio of 1.80 was computed using a Wadati diagram and is similar to values found in adjacent regions (Haessler et al., 1988, Piccinini et al., 2003). We relocated the original dataset composed of 3644 seismic events using Hypoellipse and the minimum 1-D model and obtained a final average RMS of all events equal to 0.22 s. Despite the low average RMS, we decided to further reduce the dataset in order to analyze only those events with location errors lower than ERH = 3 km and ERZ = 5 km and with azimuthal gaps lower than 270 degrees. The final dataset was composed of 1731 events of magnitudes between $2.2 < M_L < 4.4$. Their depths are mainly ranging from 0 to 15 km in the western portion and to more than 30 km in the eastern sector. The final 1-D mean formal errors of the location procedure are small. In particular, more than 80% of the events are located with a horizontal error less than 1.5 km, while the vertical errors are around 2 km. The selected dataset is shown in Figure 7.

To get a sharper and more detailed image of the individual sequences, we relocated the data of each subset applying the *double-differences* algorithm (Hypo-DD, Waldhauser and Ellsworth, 2000), using the best-fit velocity model previously obtained (Table 1). For each subset, we performed a number of iterations to optimize the damping and control parameters of the program, and to obtain good conditioning and convergence of the solution.

Fault plane solutions were calculated for all events of each subset with more than seven polarity readings. For each subset, we show the fault plane solution of three major events only (except for the *Chiusi della Verna* cluster). The stress field inversion results associated to each subset are shown in the inset of figures 3, 4 and 5.

4. Analysis of Seismicity

Figure 7a presents the epicentral map of the seismicity recorded in the Upper Tiber Valley using the previously described dataset. A closer look at the figure allows to distinguish different clusters of seismicity, in the following denominated according to the nearest town: *Pieve Santo Stefano*, *Carpegna*, *Chiusi della Verna*, *Santa Sofia*, and *Sestino*. The two clusters near *Pieve Santo Stefano* have been previously analyzed in Braun et al. (2002) and Ciaccio et al. (2007) where the authors named them as *Sansepolcro* sequences. In the ISN Bulletin the seismicity associated to the *Carpegna* cluster was reported as *Montefeltro seismicity*, jointly with the diffuse seismicity in the area. Also, the *Chiusi della Verna* cluster was not separated from the *Santa Sofia* seismicity in ISN. While these past definitions have been proven useful for a low-resolution image of Italian seismicity, we revise them here in order to avoid misinterpretations.

4.1 Pieve Santo Stefano

On 26-Nov-2001 an earthquake of M_W=4.7 occurred in the area between *Pieve S. Stefano* and *Sansepolcro* (Figure 7), followed by a two months lasting aftershock sequence. The same area was hit by a moderate seismic event of M_w = 4.4 on 29-Nov-1997 at 19:38 and a second event about two hours later with similar magnitude (M_L = 4.1). Even if the station coverage of the 1997 sequence was not optimal, we correlated the seismic sequences of 2001 and 1997, applying HypoDD to the catalogue data listed in the CSI 1.1. While the formal errors obtained for the hypocenters of the 2001 dataset (76 events) are in the range of a few tens of meters, the error reduction for the 1997 sequence is worse, resulting in a less sharp image of clustered seismicity. Figure 2 shows the epicentral map and a SW – NE cross section (A-A' in figure 1) of the 1997 and 2001 seismic sequences. The grey NE-dipping line represents the ATF, as imaged by the CROP03, located about 5 km SE of the clustered hypocenters. The focal solutions reported (green and dark red) are those reported in the RCMT database (Pondrelli *et al.*, 2002, 2004; http://www.ingv.it/seismoglo/RCMT/). We add the focal mechanism by using the first motion polarity for the 1997 second event (light red). The hypocenter pattern of the 1997 sequence developed on a SW high angle dipping structure that could be interpreted as an antithetic fault

with respect to the ATF. However, the alignment of the 2001 aftershock sequence seems to be steeper than the dip angle of the ATF. Both observations are confirmed by the focal mechanisms of the main-shocks indicating a normal fault solution. Discrepancies between the focal solutions and the aftershock distribution will be discussed later.

4.2 Carpegna

Using data from the ISN, the RSM and the CAESAR-2 networks, we analysed about 150 seismic events in the *Carpegna* area with a magnitude $M_L < 3$ (Figure 3) in the period between from 15-sep-2005 to 15-oct-2005. Despite the final RMS is small (0.17 s), and the formal location errors are even small (ERH < 1 km; ERZ < 2 km), the seismicity distribution does not show any clear geometrical pattern. Therefore, the local seismicity of the *Carpegna* area appears to be substantially different from the other clusters described in the present paper and, in general, from the seismicity commonly located along the inner part of the western side of the Apenninic chain (Tuscany). Although we cannot exclude the possibility of the occurrence of large earthquakes in this area, we observe that diffuse crustal seismicity seems to be a behavior of the inner part of the study area (i.e. Val Tiberina Basin). However, microseismicity release in the *Carpegna* area, and more in general of the Marche area, is observed at noticeably greater depths than the on the Tuscan side. We observe that the main part of the *Carpegna* cluster seismicity is released in the deeper part of the upper crust (Z > 10 km), down to the lower crust (Piana Agostinetti et al. 2002; Levin et al. 2002). The magnitude range of the recorded seismic events lies between $1 < M_L < 3$, the seismicity extends almost vertically, and seems not to be related to any fault structure.

Focal mechanisms of the three major events ($M_L > 2$) are shown in Figure 3a, plotted together with local stress axes retrieved from the inversion of 52 focal mechanisms of the complete seismic sequence. We also computed the stress axis of a subset of deeper events (Z > 12 km) . Focal mechanisms and stress axes for the complete seismic sequence show coherent directions: the major stress axis σ_1 is almost horizontal and oriented NW, while σ_3 lies in the horizontal plane (strike slip solution). We notice that the analysis of the deeper events shows a different stress configuration. In fact, for depths greater than 12 km the two minor stress axis switch their position, while the major stress axis remain unchanged. The resulting stress field is compressive although the major stress axis is parallel to the strike of the compressive structures of the area.

232

233 **4.3 Chiusi della Verna**

234 A small seismic sequence composed of 29 small events ($M_L < 2.3$) was localized at the beginning
235 of October 2005 near the small town *Chiusi della Verna* (Figure 4). The cluster is well confined
236 in space and time, and about 80% of the events occurred within the subsequent 18 hours. Due to
237 the lack of a main shock, a composite focal mechanism was calculated using the first arrival
238 polarities of the sequence. We also inverted the stress field obtained by using 19 focal solutions.
239 The resulting major stress axes are partly in agreement with the regional stress field, showing an
240 almost vertical σ_1, and a σ_3 axis orthogonal to the regional one. Due to the very small magnitude
241 we do not discuss in detail this peculiarity of our results even if we suggest the possibility of a
242 local rearrangement of the regional stress field.

243

244 **4.4 Santa Sofia**

245 On 26-Jan-2003 two moderate earthquakes of M_L=4.3 hit the Santa *Sofia* area. Both events
246 occurred within a time span of less than 20 minutes. As evident from the seismicity distribution
247 (Figure 5) both main shocks occurred in the same crustal volume at a depth of about 10 km. The
248 resulting location errors are small (RMS=0.10) and the seismicity distribution imaged by the
249 seismic cross-sections shows a SW dipping structure. This is in good agreement with the two
250 normal fault solutions (Figure 5), indicating one of the fault plane dipping between about 40 and
251 60 degrees towards SW. The composite fault plane solution of the sequence is quite similar to the
252 two major events with an almost pure normal fault mechanism. The stress field inversion
253 obtained inverting the available fault plane solutions indicates direction and plunge of the stress
254 axes to be equivalent to those of the regional stress field. Although the Santa Sofia area is located
255 in the outer sector of the chain, its stress field could be correlated to the extensional regime
256 present in the inner part of the chain itself.

257

258 **4.5 Sestino**

259 During a five months operation period, the CAESAR-1 network recorded an earthquake swarm
260 of more than 250 events. Most of the events were too small to be recorded by more than two

stations of the network and hence we locate the events using only S-P time and first arrival particle motion. Although we could not estimate the error location, we observed that the earthquakes occurred within a sort time span of only 26 hours and originated from a spatially restricted area about 5 km south of station RSP (asterisk in figure 6). In fact, a closer look on the records indicates that most of the recorded seismicity shows high waveform similarities and virtually identical S-P delay times (figure 6). These are strong indications for a co-location of the seismic sources and similar source mechanisms of the events. Moreover, the generally small energy released by the single earthquakes and the lack of a typical mainshock-aftershock pattern lead us to speculate that the swarm earthquakes could have been generated within a relatively small source volume, such as a creeping fault patch. They behave as repeating earthquakes (repeaters), i.e. earthquakes of similar size located in the same area which repeatedly rupture the same fault section (Waldhauser et al., 2004).

5. Discussion and conclusions

In the present study we review the seismicity of the Upper Tiber Valley, using datasets combined from temporary local seismic experiments and the RSM and INGV-databases. Five distinct clusters of moderate earthquakes have been observed and localized during the last 10 years (from SE to NW): *Pieve S. Stefano* (A1, A2), *Carpegna* (B), *Chiusi della Verna* (C) and *S. Sofia* (D). Figure 7b shows the depth and spatial distributions of the clusters plotted on two normal sections. The clusters A1-A2, C, D lie exactly on the Apenninic orientated section line (Figure 7b), while cluster A1-A2 and B are situated along the anti-Apenninic section line (Figure 7b). The *Sestino* cluster lies in the midway between clusters A1-A2 and B, along the section line in Figure 7b.

Comparative observation of the peculiarities of each cluster and their spatial distribution, together with the position of the historical earthquakes, suggests the following characterization of the Upper Tiber Valley seismicity: In the outer part of the Apenninic chain (Marche side), the seismicity distribution of B (Figure 3 and 7b) reaches depths of ~30 km and our dataset suggests a switching of the stress field from transpressive to almost compressive at depths greater than 12 km. Although the small magnitude events poorly constrain the stress inversion results, stress rotation with depth is a behavior known from adjacent areas of the Apenninic chain. For example Piccinini et al., 2006 interpreted the compression evidence of the *Monghidoro* seismic sequence

(Northern Apennines) as a secondary process caused by differential motion inside the flexed Adriatic lithosphere. In this way an explanation could be given, why thrust fault mechanisms are observed close to the extensional belt of the Apennines (e.g. *Mugello* basin).

However, near the inner part of the chain (Tuscan side), the hypocentres of A1-A2 are almost completely confined in the upper crust. In particular, the seismicity distribution of these clusters suggests that the ATF continues towards the northern part of the study area, acting as the lower boundary for the seismic energy release. The seismicity of the 1997 and 2001 sequences seems to be confined in the hanging wall block of the fault in agreement with previous studies (Boncio et al., 2000, Collettini and Barchi, 2002, Piccinini et al. 2003 and Chiaraluce et al., 2007). These authors report that the diffuse seismicity in the southern adjacent area is confined in depth by the ATF. The pattern found for the hypocenters of the 2001 sequence indicates that the ATF continues also in the NW part respect to the CROP03 line. Comparing our locations to those previously proposed (Braun et al., 2002, Ciaccio et al. 2007), we motivate the clustering of the seismicity due to the use of different data and location methods. From the located earthquakes distribution we prove the presence of two antithetic faults (Figure 2 and 7c) limited in depth by the presence of the ATF. The discrepancy between the seismicity distribution and the focal mechanisms could be caused either to a mislocation of the seismic sequence, or to a badly constrained focal solution, obtained by using different methods (see section 4.1 for details). Analyzing the fault geometry obtained by relocating the seismicity, we state that the two 1997 *Pieve Santo Stefano* mainshocks probably occurred at the intersection between the ATF and the antithetic SW high-angle dipping fault, while the aftershock sequence developed along the high-angle normal fault.

For the 2001 *Pieve Santo Stefano* seismic sequence we observed a similar discrepancy between the focal mechanism of the mainshock and the epicenter distribution of the aftershock sequence. In this case the focal solution and the CROP03 line indicates a similar dip angle of the ATF, while the aftershock locations align along a steeper plane. A plausible explanation for this observation could be, that the aftershock sequence involved one of the steeper and shallower splays of the ATF.

On the midway between the *Pieve Santo Stefano* and *Carpegna* clusters, we observed the microseismicity associated to the *Sestino* cluster, described in Section 4.5 asterisk in Fig. 7). The

presence of a low-magnitude microseismicity in the *Sestino* area suggests that the seismic energy release in this area could be associated to a small source volume able to generate earthquakes of similar size which repeatedly rupture the same fault section.

In our analysis we demonstrated that the seismic energy release across the Apenninic chain occurs in different matters. Some critical peculiarities become evident when looking at the spatial and temporal distribution along the chain. As shown in Figure 7b the seismicity clusters of profiles A1-A2, C, D (compare fig. 1) are confined in the upper crust and their observed maximum depths are 9 km, 13 km and 18 km, respectively, showing increasing depths from SE to NW. Looking at the historical seismicity (Figure 7a and 7b), the strong earthquakes seem to be spatially grouped. Independent of their time of occurrence, we distinguish the following historical clusters that lie near the section E-E': H1 (*Gualdo Tadino*), H2 (*Sansepolcro*), H3 (*S. Sofia*). While the diffuse microseismicity of *Città di Castello* falls exactly between H1 and H2, the moderate earthquakes plus aftershock sequences A, C, D occurred in an area with a low seismicity release, between H2 and H3. In particular, we observe that two zones along the Apenninic chain do not display any of the three previously illustrated modes of seismic energy release, i.e. neither a high level of microseismicity, nor moderate sequences nor stronger historical earthquakes. Between *Città di Castello* and the H2 events, we localized fewer seismic events compared to the frequency of small earthquakes in the southernmost part of the study area. Between the clusters A1-A2 and C, neither instrumental seismicity nor stronger historical earthquakes are present.

Finally the stress field, resulting from the inversion of fault plane solutions for each individual cluster along the profile E-E', depict an homogeneous and unexpected image. Results from the cluster A1-A2 (*Pieve Santo Stefano*) are in agreement with the extensional regime interesting the inner part of the Apenninic chain. On the other hand retrieved stress fields for clusters C (*Chiusi della Verna*) and D (*Santa Sofia*) show a near vertical $\sigma 1$, suggesting the presence of the extensional regime beyond the Apenninic watershed towards the Adriatic sea, where compressive regime is expected.

Acknowlegdements:

We are grateful to T. Plenefisch, K. Klinge, R. M. Azzara, F. Bergamaschi, M. Ohrnberger, F. Krüger, and D. Vollmer for the help during field work. Part of the work was supported by the Deutsche Forschungsgemeinschaft (KL 776/4-1) and by the Regione Toscana (Convenzione Valtiberina). Useful suggestions to improve the paper were given by P. Boncio, L. Chiaraluce and an anonymous referee.

Bibliografia

Alvarez, W. (1972), Rotation of the Corsica-Sardinia microplate, *Nature*, **248**, 309– 314.

Azzara, R., P. Augliera, F. Bergamaschi, T. Braun, E. D'Alema, D.D. Giacomo, S. Marzorati, M. Massa, N. Piana Agostinetti & P. Roselli (2006): Un array lineare fra Sansepolcro e Anghiari (Alta Valtiberina): acquisizione dati e prime analisi da terremoti e microtremore. (2006) *Atti 25° Convegno G.N.G.T.S., 28.-30.Nov. 2006*, Roma/Italy.

Bally, A. W., L. Burbi, C. Cooper, and R. Ghelardoni (1986). Balanced sections and seismic reflection profiles across the central Apennines, Mem. Soc. Geol. Ital. **35**, 257–310.

Barchi M.R., A. De Feyter A., Magnani M.B., Minelli G., Pialli G. e Sotera B.M.; (1998): Extensional tectonics in the Northern Apennines (Italy): Evidence from the CROP03 deep seismic reflection line. *Mem. Soc. Geol. It.*, **52**, 527-538.

Boncio P., Brozzetti F. and Lavecchia G. (2000) - Architecture and seismotectonics of a regional Low Angle Normal Fault zone in Central Italy. *Tectonics*, **19**, 1038-1055.

Boncio P. and Lavecchia G., (2000), A structural model for active extension in Central Italy, *J. of Geod.*, 29, 233-244, doi:10.1016/S0264-3707(99)00050-2

Braun T., C. Chiarabba, M.G. Ciaccio, F. Di Luccio e D. Piccinini (2002): Evidenze di attività sismica sulla faglia Altotiberina. *Atti 21° Convegno G.N.G.T.S., 19.-21. Nov. 2002, Roma/Italy.*

Braun T., T. Dahm, F. Krüger, M. Ohrnberger & F. Scherbaum (2006): Seismic array analysis of Tornillo-like signals recorded in Tuscany. *Atti 25° Convegno G.N.G.T.S., 28.-30.Nov. 2006, Roma/Italy.*

Chiarabba C., Jovane L, and Di Stefano R. (2005). A new view of Italian seismicity using 20 years of instrumental recordings", *Tectonophysics*, **3,** 251-268

Chiaraluce L., C. Chiarabba, C. Collettini, D. Piccinini, and M. Cocco (2007) Architecture and mechanics of an active low-angle normal fault: Alto Tiberina Fault, northern Apennines, Italy, *J. Geophys. Res., doi:10.1029/2007JB005015*

Ciaccio M.G., Pondrelli S., Frepoli F., (2007) Earthquake fault-plane solutions and patterns of seismicity within the Umbria Region, Italy, *Ann. Geophysics*, **49** (4/5), 987-1002.

Ciaccio M.G., Mirabella F., Chiarabba C., Barchi M.R. and Stucchi E. (2005). Seismological, geological and geophysical constraints for the Gualdo Tadino Fault, Umbria-Marche Apennines (Central Italy). *Tectonophysics*, **406/3-4**, 233-247.

Collettini, C., and M. R. Barchi (2002), A low angle normal fault in the Umbria region (central Italy): A mechanical model for the related microseismicity, *Tectonophysics*, **359**, 97-115.

Deschamps, A., D. Iannaccone, and R. Scarpa (1984). The Umbrian earthquake (Italy) of 19 September 1979, *Ann. Geophys*. **2**, no. 1, 29–36.

394 Guidoboni E., G. Ferrari, D. Mariotti, A. Comastri, G. Tarabusi and G. Valensise (2007)
395 CFTI4Med, Catalogue of Strong Earthquakes in Italy (461 B.C.-1997) and Mediterranean
396 Area (760 B.C.-1500). INGV-SGA. *Available from http://storing.ingv.it/cfti4med/*

397 Haessler, H., R. Gaulon, L. River, R. Console, M. Frogneaux, G. Gasparini, L. Martel, G. Patau,
398 M. Siciliano, and A. Cisternas (1988). The Perugia (Italy) earthquake of 29 April 1984: a
399 microearthquake survey, *Bull. Seism. Soc. Am*. **78**, no. 6, 1948–1964.

400 Hunstad, I., G. Selvaggi, N. D'Agostino, P. England, P. Clarke, and M. Pierozzi (2003). Geodetic
401 strain in peninsular Italy between 1875 and 2001, *Geophys. Res. Lett*. **30**, no. 4, 1811.

402 Kissling, E.,W.L. Ellsworth, D. Eberharth-Phillips and U. Kradolfer (1994): Initial reference
403 model in local earthquake tomography, *J. Geophys. Res.*, **99**, 19635-19646.

404 Lahr, J.C., (1989). HYPOELLIPSE/Version 2.0: A computer program for determining local
405 earthquakes hypocentral parameters, magnitude, and first-motion pattern. *US Geological*
406 *Survey Open-File Report* 89-116, online edition.

407 Levin V., L. Margheriti, J. Park, and A. Amato (2002): Anisotropic seismic structure of the
408 lithosphere beneath the Adriatic coast of Italy constrained with mode-converted body
409 waves, *Geophys. Res. Lett*., **29 (22)**, 2058, doi:10.1029/2002GL015438.

410 Michael, A. J., (1984), Determination of stress from slip data: faults and folds. *J. Geophys. Res.*,
411 **89**, 11517-11526.

412 Montone, P., M. T. Mariucci, S. Pondrelli, and A. Amato (2004), An improved stress map for
413 Italy and surrounding regions (central Mediterranean), *J. Geophys. Res*., **109**, B10410,
414 doi:10.1029/2003JB002703.

415 Pialli, G., M. Barchi, and G. Minelli (1998), Results of the CROP03 deep seismic reflection
416 profile, Mem. **52**, 657 pp., *Soc. Geol. Ital.*, Rome.

417 Piana Agostinetti, N., F. P. Lucente, G. Selvaggi, and M. Di Bona, (1999) Crustal Structure and
418 Moho Geometry beneath the Northern Apennines (Italy) *Geophys. Res. Lett*., **29 (20)**,
419 1999, doi:10.1029/2002GL015109

420 D. Piccinini, C. Chiarabba, P. Augliera and MEG (2006): Compression along the northern
421 Apennines? Evidence from the Mw 5.3 Monghidoro earthquake, *Terra Nova*, **18**, 2, 89-
422 94, doi:10.1111/j.1365-3121.2005.00667.x

423 Piccinini, D., Selvaggi, P. Augliera, D. Spallarossa, G. Ferretti, A. Michelini, A. Govoni, P. Di
424 Bartolomeo, M. Romanelli and J. Fabbri (2003): A microseismic study in a low seismicity
425 area of Italy: the Città di Castello 2000-2001 experiment. *Ann. Geophysics*, **46** (6), 1315-
426 1324.

427 Pondrelli, S., A. Morelli, G. Ekström, S. Mazza, E. Boschi and A.M. Dziewonsky (2002):
428 European-Mediterranean regional centroid-moment tensors: 1997-2000, *Phys. Earth*
429 *Planet. Int.*, **130**, 71-101.

430 Pondrelli, S., A. Morelli and G. Ekström (2004): European-Mediterranean regional centroid-

moment tensor catalog: solutions for years 2001 and 2002, *Phys. Earth Planet Inter.*, **145**, 127-147

Reasenberg, P. and D. Oppenheimer (1985): FPFIT, FPPLOT and FPPAGE: FORTRAN computer programs for calculating and displying earthquake fault-plane solutions, *U.S. Geol. Surv. Open-File Rep. 85-739*.

Reutter, K. J., P. Giese, and H. Closs (1980), Lithospheric split in the descending plate: Observations from the northern Apennines, Tectonophysics, **64**, T1– T9.

Waldhauser, F., and W. L. Ellsworth (2000): A double-difference earthquake location algorithm: Method and application to the northern Hayward Fault, California. *Bull. Seismol. Soc. Am.*, **90**, 1353– 1368.

Waldhauser, F., W. L. Ellsworth, D. P. Schaff, and A. Cole (2004): Streaks, multiplets, and holes: High-solution spatiotemporal behavior of Parkfield seismicity. *Geophys. Res. Lett.*, **31**, L18608, doi:10.1029/2004GL020649

Westaway, R., Gawthorpe, R., Tozzi, M., (1989): Seismological and field observations of the 1984 Lazio –Abruzzo earthquakes: implications for the active tectonics of Italy. G. J. Int. **98**, 489– 514.

448 **Figure Captions**

449 **Figure 1:** Introductive map of the study area. Seismic stations used in the study are represented by
450 triangles and labelled by colors: gray/red framed - ISN, yellow - CAESAR-1 (2002-2003), blue -
451 AVESA (2005), red - LASES (2005), green - CAESAR-2 (2005-2006). Black solid lines represents
452 the cross sections described in the text. The gray bold solid and dashed line represents the part of
453 the CROP03 interesting the area, while the outcrop of the ATF and its hypothetical continuation
454 towards NW (EFS) are plotted in solid/dotted red, respectively. Names of the geographic regions
455 and cities are represented in bold gray. Orange stars represents the locations of the historical
456 earthquakes discussed in the text.

457 **Figure 2**: Seismicity distribution of the *Pieve Santo Stefano* clusters shown as map and cross
458 section in SW-NE direction (A-A'): 1997 and 2001 hypocenters are represented with red and green
459 dots, respectively. Focal mechanisms for the mainshocks of 1997 (dark red for QRCMT of the first
460 event - M_w = 4.4, light red for the polarity inversion of the second event - M_L = 4.1) and the
461 mainshock of 2001 (green QRCMT for the M_w = 4.7). The projection of the position of the ATF, as
462 evidenced by CROP03, is plotted in light gray.

463 **Figure 3:** Map and cross section showing the seismicity distribution of the *Carpegna* cluster.
464 Different colors indicate the two subsets used for the stress field inversion. The focal solution of the
465 three strongest events of the sequence (M_L > 2.6) is represented in black. Notice the direction of the
466 principal stress axis (inset): in light blue are plotted the directions derived from the entire dataset, in
467 dark blue those retrieved from the focal solution of the deeper events (see detail in the text).

468 **Figure 4:** Map and cross section for the *Chiusi della Verna* cluster (yellow dots). Cumulative focal
469 solution and direction of principal stress axis in maps are shown.

470 **Figure 5:** Map and cross section of the *Santa Sofia* earthquake cluster of 2003 (light blue dots). The
471 focal solution of the two larger events are shown in black. The insets represents the cumulative
472 focal solution for the dataset and the direction of the principal stress axis derived from the focal
473 mechanisms.

474 **Figure 6:** Waveform similarity of events registered at station RSP. The filtered (4 - 25 Hz)
475 Waveforms recorded on the vertical component are aligned using a cross correlation algorithm over

476 0.4 s around the P-wave arrival time. Only those waveforms with a cross-correlation index greater
477 than 0.9 are shown.

478 **Figure 7**: The epicenters of the data set between 1997 and 2006 are represented by small dots: A)
479 *Pieve S. Stefano* 1997 and 2001 (red and green), B) *Carpegna* (blue), C) *Chiusi della Verna*
480 (yellow), D) *Santa Sofia* (light blue), the background seismicity around *Città di Castello* (black),
481 and CSI catalogue seismicity (light grey). The *Sestino* seismicity is represented by a black asterisk.
482 Cross-sections showing the seismicity distribution in the Upper Tiber Valley along the NW-SE
483 direction (E-E') and SW-NE direction (F-F') are also shown. The fault plane solutions of the events
484 with magnitude larger than M = 4 are plotted by colored beach balls.

Figure 1

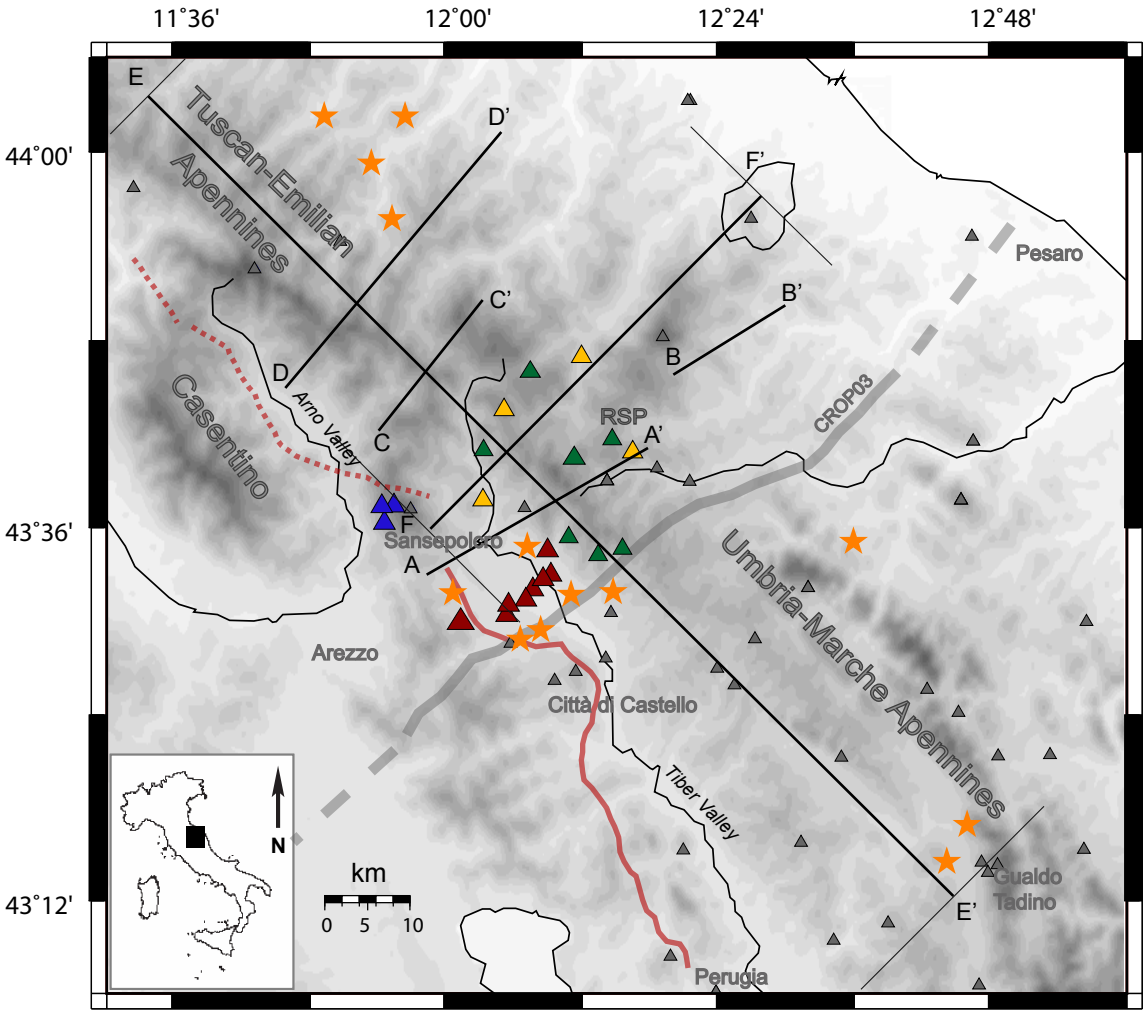
11°36'
12°00'
12°24'
12°48'
44°00'
43°36'
43°12'
E
D'
F'
C'
B'
B
D
C
A'
F
A
E'
Tuscan-Emilian Apennines
Casentino
Arno Valley
RSP
CROP03
Pesaro
Sansepolcro
Umbria-Marche Apennines
Arezzo
Città di Castello
Tiber Valley
Gualdo Tadino
Perugia
N
km
0 5 10

Figure 2

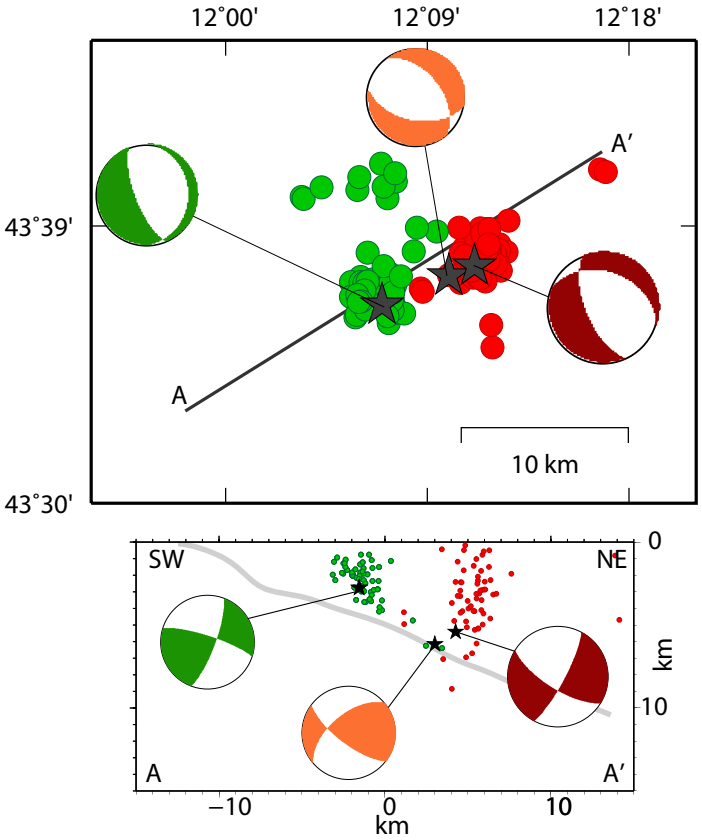

Figure 3

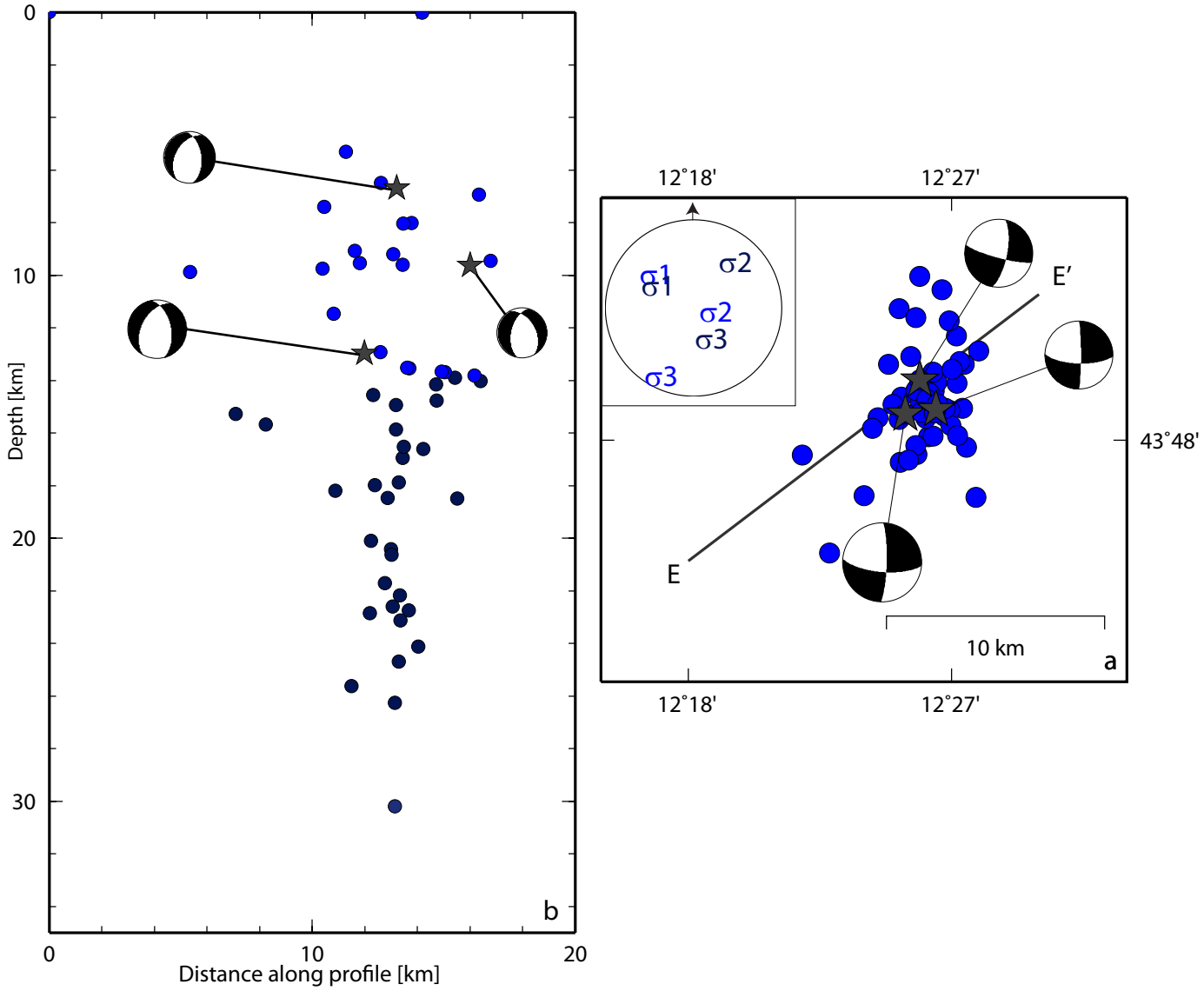
0
10
20
30
Depth [km]
0
10
20
Distance along profile [km]
b
12°18'
12°27'
σ1
σ2
σ1
σ2
σ3
σ3
E′
E
43°48'
10 km
a
12°18'
12°27'

Figure 4

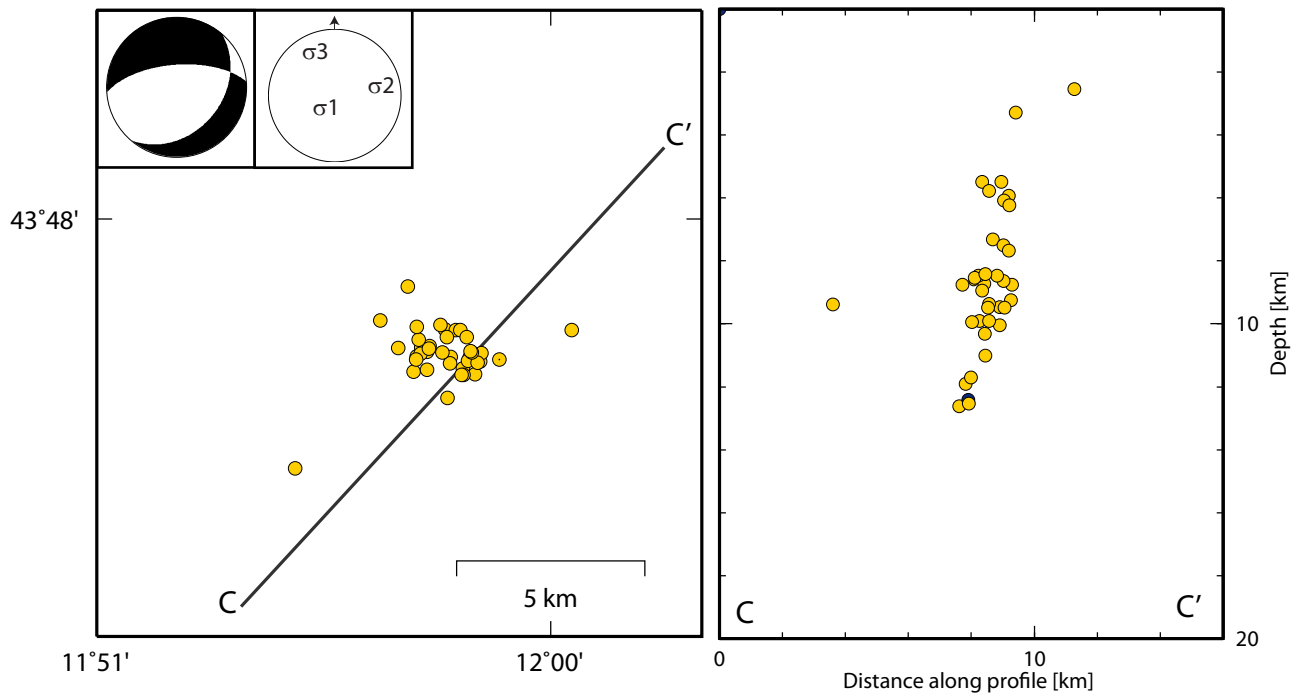
σ3
σ2
σ1
C′
C
43°48'
5 km
11°51'
12°00'
C
C′
0
10
Distance along profile [km]
10
20
Depth [km]

Figure 5

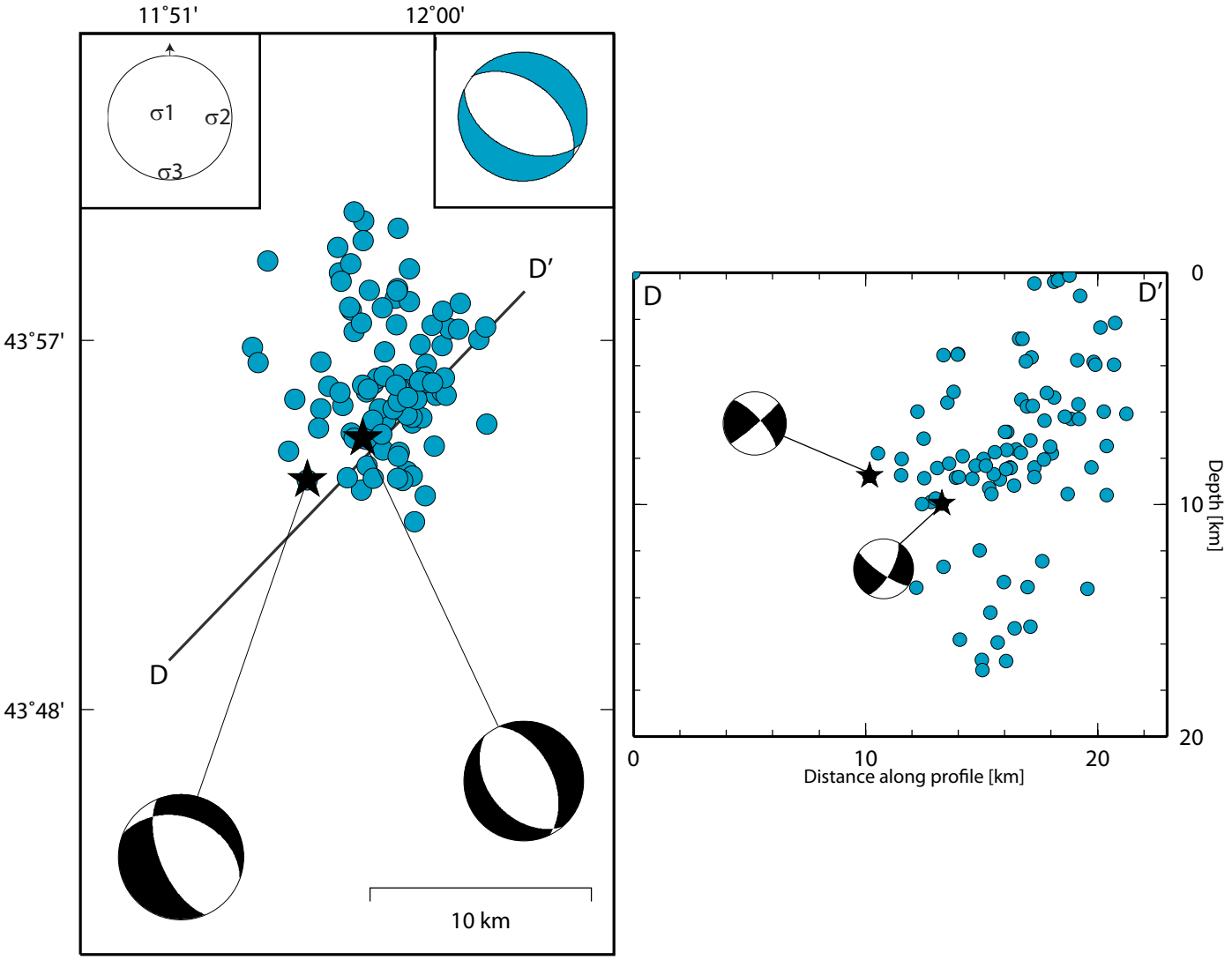
11°51'
12°00'
σ1
σ2
σ3
43°57'
43°48'
D
D′
10 km
D
D′
0
10
20
Depth [km]
0
10
20
Distance along profile [km]

Figure 6

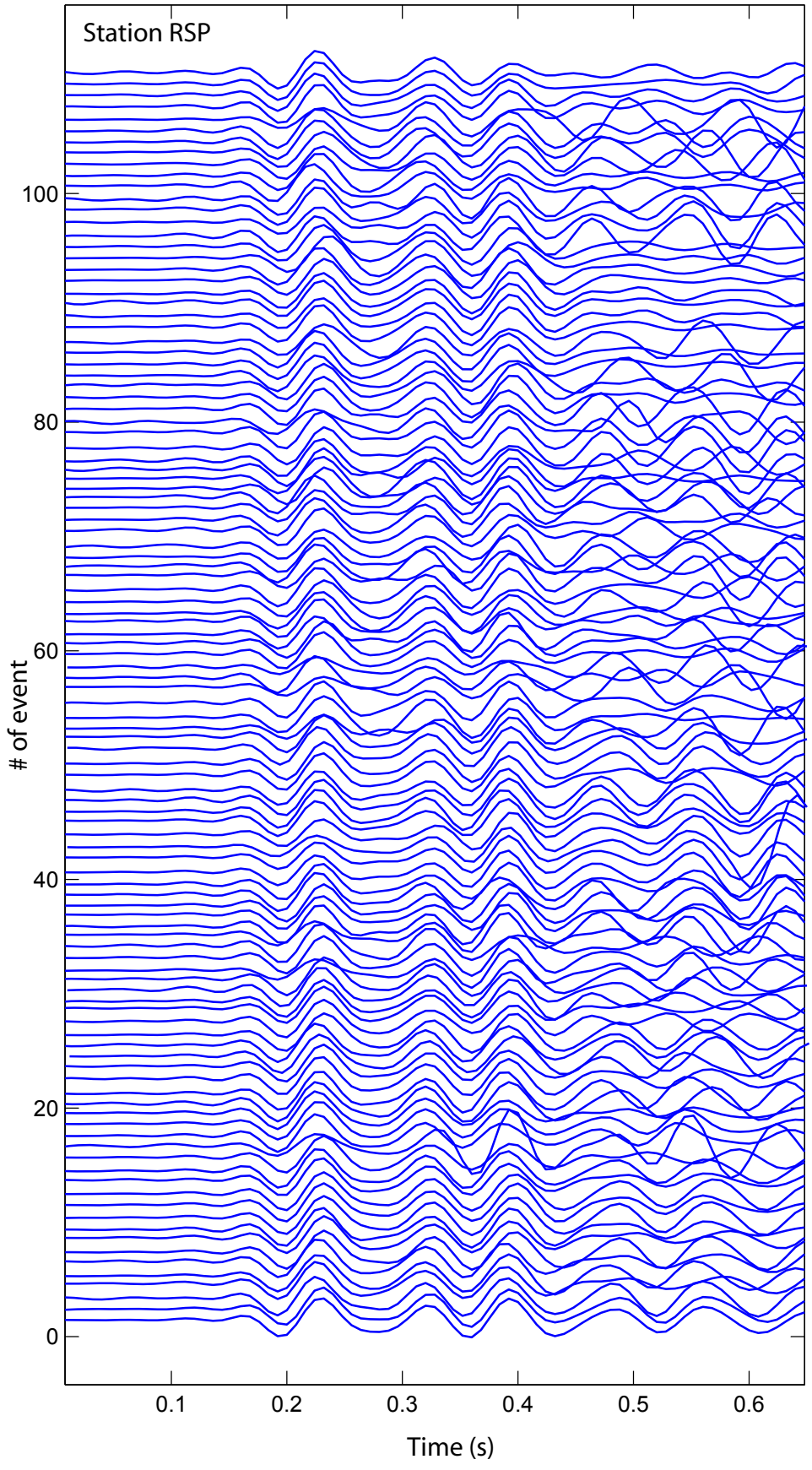

Figure 7

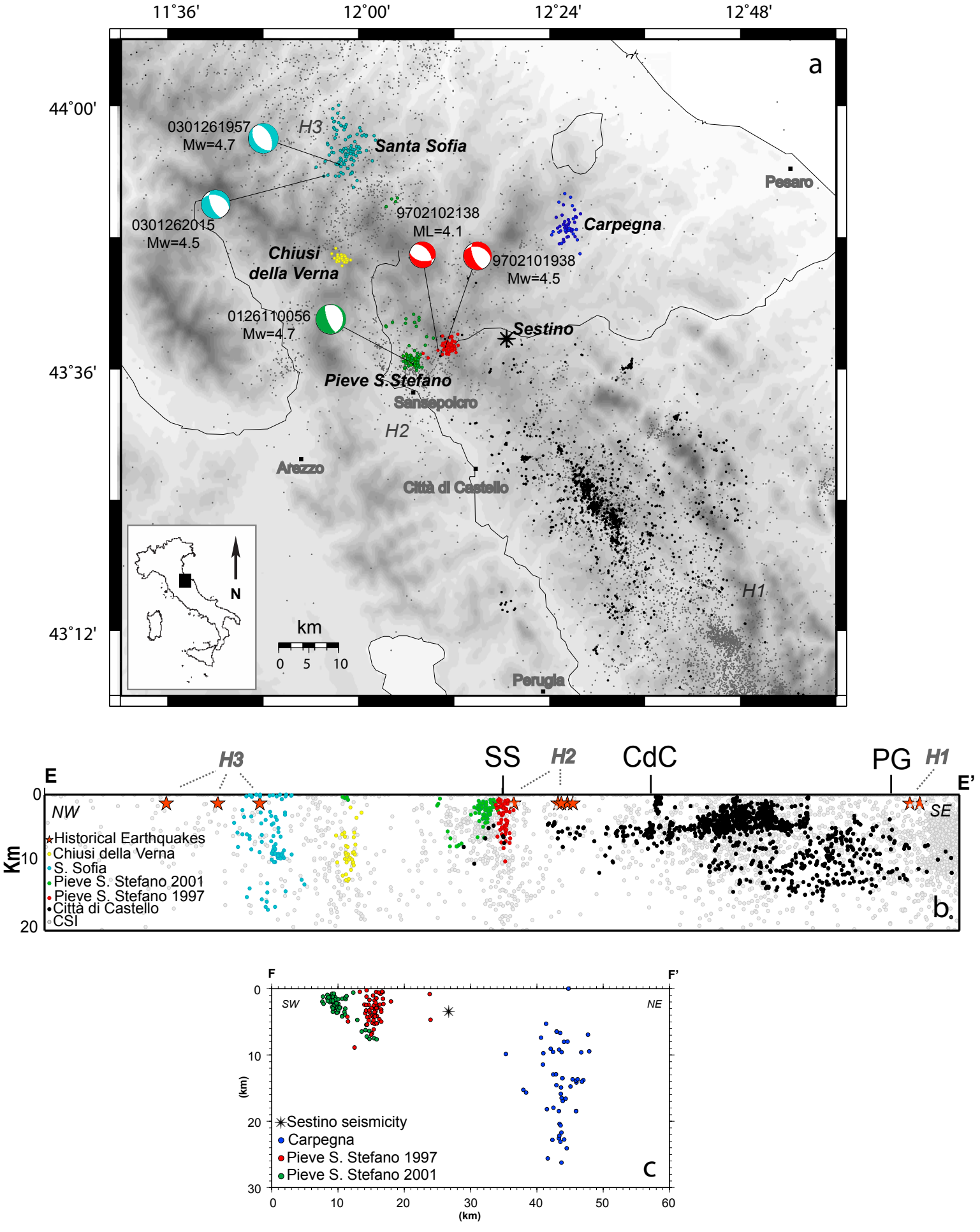
11˚36'
12˚00'
12˚24'
12˚48'
44˚00'
43˚36'
43˚12'
a
0301261957
Mw=4.7
H3
Santa Sofia
0301262015
Mw=4.5
9702102138
ML=4.1
9702101938
Mw=4.5
Carpegna
Pesaro
Chiusi
della Verna
0126110056
Mw=4.7
Sestino
Pieve S.Stefano
Sansepolcro
H2
Arezzo
Città di Castello
H1
N
km
0 5 10
Perugia
E
E'
H3
SS
H2
CdC
PG
H1
0
10
20
Km
NW
SE
Historical Earthquakes
Chiusi della Verna
S. Sofia
Pieve S. Stefano 2001
Pieve S. Stefano 1997
Città di Castello
CSI
b
F
F'
SW
NE
(km)
Sestino seismicity
Carpegna
Pieve S. Stefano 1997
Pieve S. Stefano 2001
c

Table 1
Click here to download Table: Table1.pdf

Table 1:

Vp (km/s)	Depth (km)
5.200	0.0
5.700	1.0
5.900	4.0
6.100	6.0
6.200	8.0
6.400	10.0
7.800	34.0